

CFD COMPUTATION OF THE GROUND EFFECT ON AIRPLANE WITH HIGH ASPECT RATIO WING

Sun Tae Kim*, Youngtae Kim**, Tae Kyu Reu*

*Agency for Defense Development, **Korean Air R&D Center

kim_st90@hanmail.net; ytkim99@hanmail.net; reut@add.re.kr

Keywords: Computational Fluid Dynamics, Ground Effect, High AR Wing

Abstract

Ground effect is an important aerodynamic characteristics during the take-off and landing for airplane with high aspect ratio wing. In order to understand the ground-effect on airplane, it is necessary to determine when aircraft is flying close to ground. Numerical study on the ground effect around high aspect ratio airplane is done using commercial CFD software FLUENT.

In this study, aerodynamic characteristics of lift, drag, and pitching moment about vehicle on both ground effect and free-air are compared with. Also the result of predicting ground effect using engineering experimental method of ESDU(Engineering Science Data Unit) and Aerospace Handbook are added to the CFD result. Aerodynamic contribution and interaction of aircraft components with respect to angle of attack are extracted from CFD result.

1 Introduction

It has long been recognized that flight close to a boundary surface is more aerodynamically efficient than flight in the free stream. Ground effect is the phenomenon caused by the presence of a boundary below and near a wing. The boundary alters the flow of the air around the wing, causing an increase in the lift of the wing and a reduction in the induced drag of wing. The effect becomes more pronounced as the wing gets close to the boundary. Fig. 1 depicts a wing in ground effect. The boundary creates an alteration of the flow field that is caused by the boundary not allowing the flow under the wing to expand as it would in free air. The total pressure of the flow field can be

divided between the static pressure and the dynamic pressure. As the total pressure remains constant throughout the flow field, the sum of the static and the dynamic pressure must also remain constant. As the flow is forced into the region between the wing and the boundary, the decrease in the dynamic pressure is transformed into a rise in the static pressure. This rise in the static pressure is often referred to as 'ram pressure'. The resulting altered pressure distribution causes a net increase in the lift and a change to many of the other aerodynamic characteristics of the wing [1, 2].

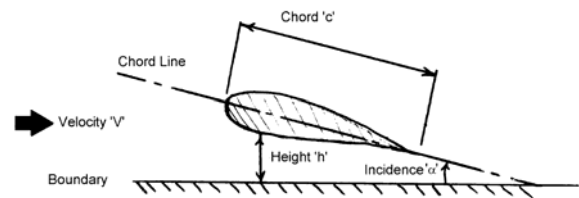


Fig. 1. Wings in Ground Effect[1]

Ground-effect prediction has been a challenging problem for many reasons. Analytical methods have generally been based on steady-state flow superposition and engineering methods such as panel codes[3,4]. These methods have limited ability to incorporated configuration complexity such as high-lift system details and the modeling of engine exhaust flows. Wind-tunnel testing often has similar limitations and might invoke additional complications. A moving ground belt or other devices are often needed to remove the unrealistic boundary layer on the wind-tunnel ground plane simulation, Several studies have also attempted to include dynamic effects[5,6,7].

Although flight tests might provide data to validate the performance of the predictive methods, these measurements are difficult to

obtain. The parametric variations are limited when an airplane is flown in close proximity to ground. The airplane must be kept close to trim, and sink rates must be controlled to avoid overstressing the landing gear. Flight measurements can be obtained in both steady-state (level flight over the ground) and dynamic (descending flight path similar to landing) conditions; however, relating the ground-effect increments to a reliable out-of-ground effect reference condition can be difficult. Because ground-effect increments are relatively small compared to other airplane forces and moments, even small atmospheric disturbances can affect the quality of the flight data. Any wind across the runway has a boundary layer, or varying velocity profile, that will provide a systematic error in the ground-effect measurements.

Using method based upon Lanchester-Prandtl theory, Wieselsberger had performed numerical simulation of aerodynamic relations between wing and ground effect [8]. Matthew, et al had done the three dimensional viscous analysis of the full airplane in ground effect with using OVERFLOW code[9] and compared to wind tunnel photographs and data[10].

In this study, we have focused the numerical analysis of ground effect on the landing configuration of the airplane with high aspect ratio wing using commercial S/W Fluent [11] and compared with the semi-empirical predictions which can consider wing alone.

2 Computational Grids and Flow Conditions

In order to generate the computational grids of the airplane with high aspect ratio wing in Fig. 2, commercial grid software ANSA was used. For the current simulations, half the airplane was meshed with a symmetry plane and no sting. In total, the flow domain around half-span configuration contains unstructured grid cells of approximately 15 millions (7.2mil tetra plus 7.8mil prisms). In order to generate cells appropriate for the viscous computation, the height of the first cell was specified at about 0.025mm to get a y^+ close to 1. Grids of boundary layer specified at 42mm were composed of 27 prism layers with 1.2 growth rate. The grid refinements were concentrated in

the vicinity of the leading edge in order to consider the suction force as shown in Fig. 3. And three dimensional grids consist of both tetra cells (gray color) in the space and prism layers (green color) near the surface of the airplane as shown in Fig. 4.

We can see flow parameters specified in CFD code as shown in Table 1. Density-based solving option has much time consuming rather than pressure-based solver, however density-based solving is more stable and accurate in the compressible flow. By combining $k-\omega$ model near the wall and $k-\epsilon$ model off the boundary layer, $k-\omega$ SST(Shear Stress Transport) turbulent model with transitional flow which be able to reduce the computation time and to have the stability and the accuracy was used.

Boundary conditions are as below. Free stream velocity is Mach 0.2 and far boundary including inflow and outflow boundary is specified at Mach 0.2 and freestream static pressure. Flight altitude (h) is as high as 10 percentages of wing span (b) at MAC (Mean Aerodynamic Center) as shown in Fig. 5. And moving ground condition is applied as ground moved at same value of flight velocity.

General information of the airplane geometry normalized with respect to MAC is outlined in Table 2. Wing section is new laminar flow airfoil optimized according to the constraints with both thickness of 17% and L/D ratio of some target value. Wing has the dihedral angle of 3° .

To improve the convergence rate, the first order of the spatial difference scheme to obtain approximate solutions was applied. And finally the converged solutions were taken after changing the second order accuracy scheme.

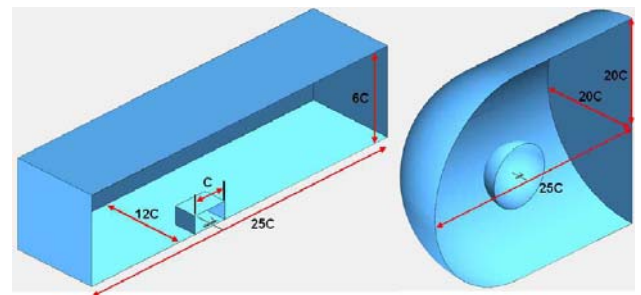


Fig. 2 Computational Domains in case of with and without Ground Effect

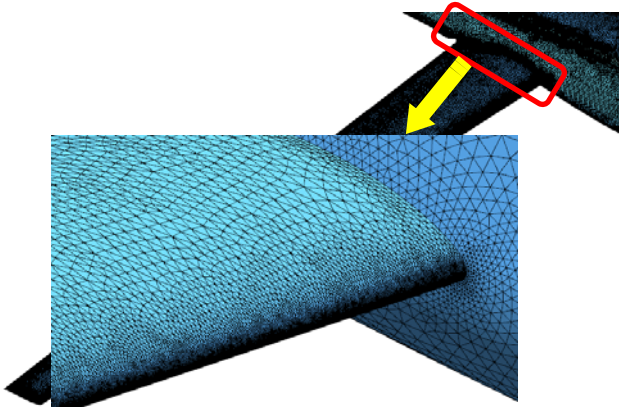


Fig. 3 Computational Surface Grids near Wing-body Junction and Leading Edge of Wing

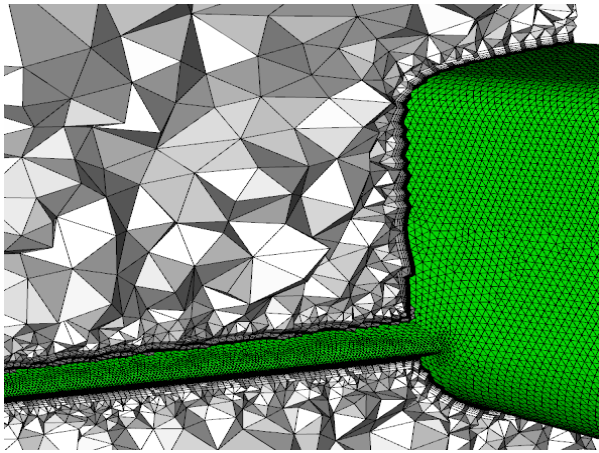


Fig. 4 Computational Volume Grids of Spatial Region and Boundary Layer

Table 1. Fluent Solver Setting[11]

Solver Option	Density-based Implicit
Turbulent Model	$k-\omega$ SST
Flux Type	Roe FDS
Discretization Scheme	Second Order Upwind
Boundary Conditions	Mach 0.2, Standard S/L
Ground Effect Height	$h/b=0.1$ (From 25% MAC)

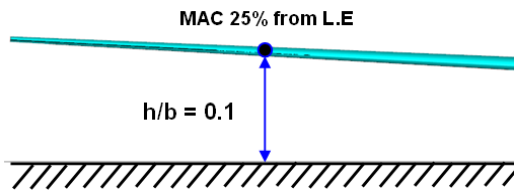


Fig. 5 Landing Configuration for considering Ground Effect (looking downstream)

Table 2. Airplane Geometry

Mean Aerodynamic Center	1.00
Wing Area	17.84
Wing Span	18.89
Aspect Ratio	20.00
Taper Ratio	0.40
Fuselage Length	9.91
Max. Equivalent Diameter of Fuselage	1.15

3 Results

3.1 Convergence Decision

Solution convergence is accomplished when the variation of drag coefficient remains less than 0.1% in the interval more than 200 iterations, then drag count is converged at level lower than 0.1. At high angle of attack we can not get the converged solutions easily due to the increase of the unsteady flow phenomena, and then we can get the converged solutions by averaging the solutions of the interval repeating at constant amplitude as shown in Fig. 6.

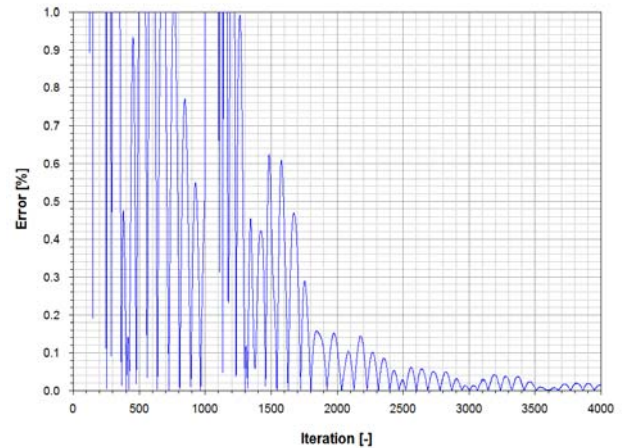


Fig. 6 Convergence History of Drag Difference

3.2 Vortex Deformation

To see the deformation of vortex due to ground effect, the ratio of local total pressure to free stream total pressure ($P_o/P_{o\infty}$) was investigated in Fig. 7. Total pressure loss is small except wake region so that total pressure ratio is confined to 0.96~1.0.

Fig.7 shows that vortex deformation at zero angle of attack has developed in ground effect and in free air respectively. Fuselage vortex

does expand a little in downstream direction and becomes strong in ground effect than in free air. It is caused by pressure rise on the lower surface of the wing in ground effect. However induced drag has not large portion in high AR wing and there is no remarkable variations of wingtip vortex.

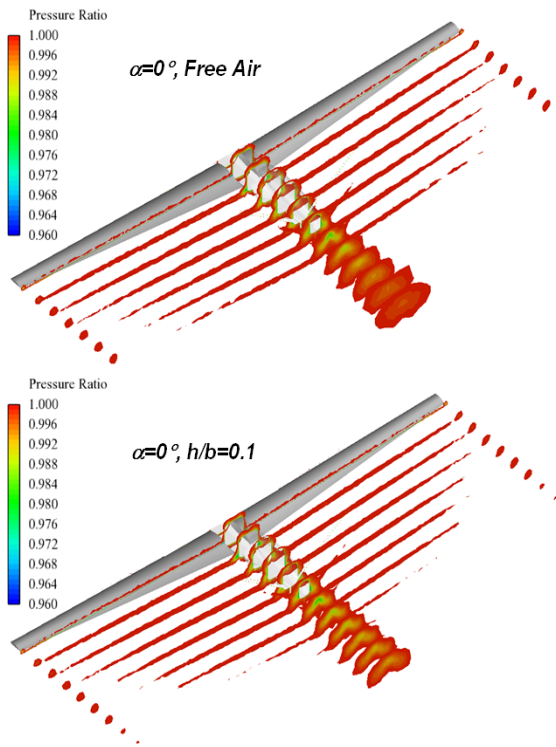


Fig. 7 Total Pressure Ratio ($P_o/P_{o\infty}$) of Airplane Wake ($M=0.2$, $Re=6.24 \times 10^6$, $\alpha=0^\circ$)

3.3 Aerodynamic Characteristics

To judge the tendency of numerical results using Fluent, we compare with the predictions of semi-empirical methods depicted such as ESDU 72023 [12] and Aerospace Handbook [13]. As shown in Fig.8, it confirmed that both CFD results and semi-empirical predictions have a similar tendency.

Ground effect has an influence on lift and drag at all angles of attack and lift increases due to pressure rise on the lower surface of the wing at relatively low angle of attack, but lift decreases at high angle of attack which flow separation happened. Induced drag diminishes due to the reduced downwash of wing.

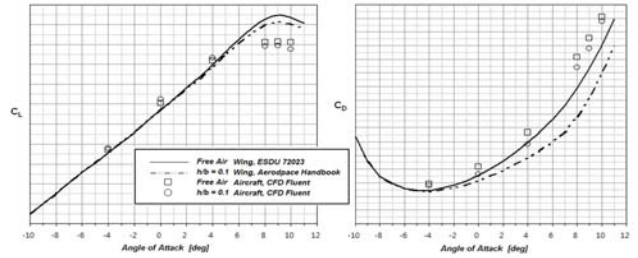


Fig. 8 Lift and Drag Coefficient at Angles of Attack ($M=0.2$, $Re=6.24 \times 10^6$)

Fig.9 shows that at zero angle of attack the distributions describe pressure coefficients at root (5%) and mid-span (43%) of wing respectively in ground effect and in free air. Pressure rise on the lower surface of the wing was done along from the leading edge to trailing edge because of ground effect.

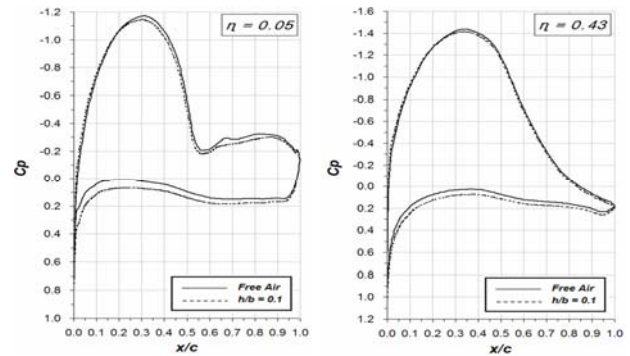


Fig. 9 Pressure Variations on Main Wing ($M=0.2$, $Re=6.24 \times 10^6$, $\alpha=0^\circ$)

Fig.10 shows that at 10° angle of attack the distributions describe the variations of pressure at root (5%) and mid-span (43%) of wing respectively in ground effect and in free air. Flow separation region becomes locally wide on the upper surface of the wing.

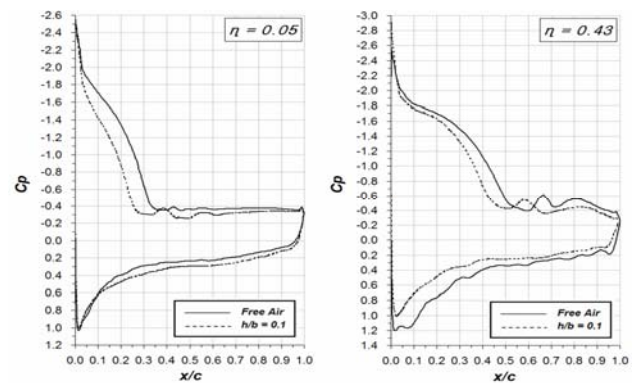


Fig. 10 Pressure Variations on Main Wing ($M=0.2$, $Re=6.24 \times 10^6$, $\alpha=10^\circ$)

3.4 Aerodynamic Contributions of Airplane Components

Fig.11 depicts the contribution of airplane components on lift generation. Most of lift is generated by the main wing. At low angle of attack lift increases due to ground effect, however more than angle of attack of 6 degrees lift decreases due to ground effect.

Fig.12 shows also the contribution of airplane components on drag generation. Drag decreases in ground effect and wing has a major part of the total drag. And at 4° angle of attack streamlines pattern on the upper surface of the wing is different between in ground effect and in free air. Downwash is smaller in ground effect than in free air. Streamlines off on the upper surface of the wing impinge against the empennage, then the contribution of the wing decreases and that of the empennage increases.

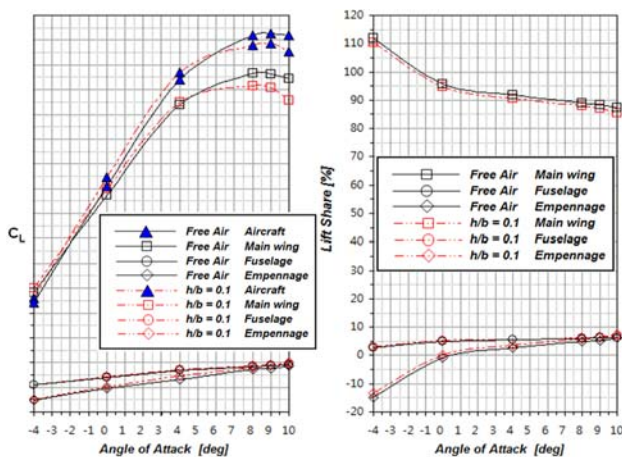


Fig. 11 Lift Characteristics of Airplane Components ($M=0.2$, $Re=6.24 \times 10^6$)

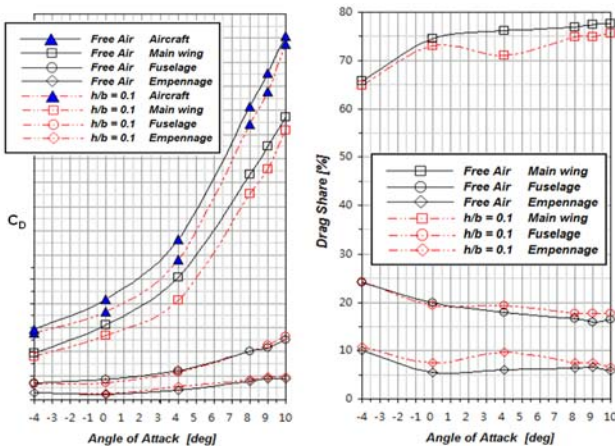


Fig. 12 Drag Characteristics of Airplane Components ($M=0.2$, $Re=6.24 \times 10^6$)

4 Concluding Remarks

This paper presents the result of numerical simulations and semi-empirical predictions on the aerodynamic characteristics around the airplane with high aspect ratio wing in ground effect. The results obtained using CFD, show a spread of integrated forces and moments over the angle of attack range considered and are compared with the semi-empirical predictions which can consider wing alone. The tendency of lift and drag altered due to ground effect is similar each other.

The semi-empirical predictions have a similar tendency to CFD results, and then it can be acceptable for prediction of drag and lift in preliminary design stage. As a method for predicting the ground effect around the airplane with high aspect ratio wing, the semi-empirical method is useful in initial design process. Because wing has a dominant role of flow phenomena around the airplane due to ground effects, the semi-empirical prediction about wing alone can be acceptable to figure out the ground effect during the landing for the airplane with high aspect ratio wing.

References

- [1] Michael Halloran and Sean O'Meara, "Wing in Ground Effect Craft Review," DSTO-GD-0201, February 1999.
- [2] Robert E. Curry and Lewis R. Owens, "Ground Effect Characteristics of the Tu-144 Supersonic Transport Airplane," NASA/TM-2003-212035, 2003.
- [3] Anderson John D., Jr., *Fundamental of Aerodynamics*, McGraw-Hill Book Company, 1984.
- [4] Hedman Sven G., "Vortex Lattice Method for Calculation of Quasi Steady State Loadings on Thin Elastic Wings in Subsonic Flow," The Aeronautical Research Institute of Sweden, Report 105, 1966.
- [5] Chen Yen-Sen and Willian G. Schweikhard, "Dynamic Ground Effects on a Two-Dimensional Flat Plate," *Journal of Aircraft*, vol. 22, no. 7, July 1985, pp.638-640.
- [6] Nuhait A. O., "Unsteady Ground Effects on Aerodynamic Coefficients of Finite Wings with Camber," *Journal of Aircraft*, vol. 32. no. 1., Jan.-Feb. 1995, pp. 186-192.
- [7] Nuhait A. O. and Zedan M. F., "Stability Derivatives of a Flapped Plate in Unsteady Ground Effect," *Journal of Aircraft*, vol. 32, no. 1, Jan.-Feb. 1995, pp.124-129.

- [8] Wieselsberger C., "Wing Resistance Near the Ground," NACA/TM-77, 1922.
- [9] Burning P. G., et al., "OVERFLOW user's Manual Version 1.7u," NASA Ames Research Center, March, 1997.
- [10] Warfield Matthew J., Treiber David A. and Wai John C., "Navier-Stokes Analysis of the DarkStar Unmanned Aerial Vehicle," AIAA-98-2530, 1998.
- [11] ANSYS FLUENT 12.0 Users Guide, April, 2009.
- [12] ESDU, "Low-speed Longitudinal Aerodynamic Characteristics of Aircraft in Ground Effect," EDSU International, Item No. 72023, 1972.
- [13] Aerospace Handbook, 2nd Edition, General Dynamics, Fort Worth Division. August 1990.

Copyright Statement

The authors confirm that they, and/or their company or organization, hold copyright on all of the original material included in this paper. The authors also confirm that they have obtained permission, from the copyright holder of any third party material included in this paper, to publish it as part of their paper. The authors confirm that they give permission, or have obtained permission from the copyright holder of this paper, for the publication and distribution of this paper as part of the ICAS2012 proceedings or as individual off-prints from the proceedings.